SCIENTIFIC REPORTS

OPEN

SUBJECT AREAS:
BIOPHYSICS
COMPUTATIONAL BIOLOGY AND BIOINFORMATICS
X-RAY CRYSTALLOGRAPHY
STRUCTURAL BIOLOGY

Received
22 March 2013

Accepted
30 April 2013

Published
15 May 2013

Correspondence and requests for materials should be addressed to T.O. (tetsuji.okada@gakushuin.ac.jp)

Common and distinct mechanisms of activation of rhodopsin and other G protein-coupled receptors

Sumire Nakamura, Takeshi Itabashi, Daisuke Ogawa & Tetsuji Okada

Department of Life Science, Gakushuin University, 1-5-1 Mejiro, Toshima-ku, Tokyo 171-8588, Japan.

Detailed and systematic examination of high-resolution structural data is a rational strategy for understanding the function of biological macromolecules. G protein-coupled receptors (GPCRs) are an exceptionally valuable superfamily of proteins for such analysis. The most intriguing question is how a variety of extracellular stimuli evoke structural changes in the intracellular surface of the receptors. The recent active-like crystal structures of GPCRs provide information for uncovering common and distinct mechanisms of light-induced and ligand-induced activation. Based on systematic structural alignment, we have analyzed 3 receptors (rhodopsin, β_2 adrenergic receptor, adenosine A_{2A} receptor) and demonstrate that the extracellular movement of helix VI is significantly different between rhodopsin and the other 2 receptors, and that the extracellular side of helix III exhibits distinct features in the 3 receptors. These findings not only emphasize the specialization of rhodopsin as a photoreceptor but also provide insights into the mechanism leading to rearrangement of helix VI.

Most of the external stimuli for eukaryotic cells, such as chemical substances, photons, neurotransmitters, and hormones are captured by G protein-coupled receptors (GPCRs), which are defined by a heptahelical transmembrane core domain. A majority of proteins in the GPCR superfamily belong to the so-called rhodopsin family, which share several key residues in their transmembrane helices. Their activity at the intracellular surface to catalyze the GDP/GTP exchange on the α-subunit of heterotrimeric G proteins is primarily determined by the type of ligand bound to the extracellular side of the transmembrane region. Even without ligand binding, GPCRs exhibit some basal activity, which is then enhanced or attenuated by binding of an agonist or inverse-agonist, respectively[1]. Antagonists are another category of ligands that maintain GPCRs in their low activity state.

Recent crystallographic studies on GPCRs have validated previous spectroscopic studies[2], demonstrating that the key intramolecular event during activation is the displacement of transmembrane helix VI at the intracellular side[3–5]. However, the manner in which this change is regulated by various ligands acting on the extracellular side is not well understood. While there are many crystallographic models of GPCRs that describe a variety of structural states of activity in the presence of different bound ligands (agonist, antagonist, and inverse agonist), systematic comparison of data obtained for different receptors has not been reported quantitatively.

Each of the crystallographic models inevitably suffers from various sources of artifacts and/or errors, as has been documented for another class of heptahelical membrane proteins, bacteriorhodopsins, whose proton pumping movement has been extensively studied using crystallographic techniques[6]. Nonetheless, statistically significant features should become apparent by averaging as many datasets as possible.

Of the more than 15 receptors of known structure, agonist-bound forms are available only for bovine rhodopsin[7–9], β_1[10] and β_2 adrenergic receptors[4,11], the A_{2A} adenosine receptor[5,12], the NTSR1 neurotensin receptor[13], the 5-HT_{1B} and 5-HT_{2B} serotonin receptors[25,26]. Unfortunately, the agonist-bound and inactive-like states are quite similar to each other in the case of the β_1 receptor. Furthermore, the structure of the NTSR1, 5-HT_{1B} and 5-HT_{2B} receptors has not yet been obtained in the inactive-like state. As a result, detailed analysis on its activation is currently feasible only for the remaining 3 receptors.

While several previous reviews on the structure of GPCRs provide a number of insights into their mechanism of activation[14–16], systematic quantitative analysis is yet to be performed. We have recently reported a rational procedure for analyzing the experimental transmembrane structures of GPCRs, based on the defined selection and superimposition of heptahelical bundles consisting of 200 residues[17]. By extending this approach, we identify previously undiscovered structural changes accompanying the activation of these receptors. The findings and the methodology will be valuable for understanding the action of ligands on other receptors of unknown structure.

Table 1 | PDB entries used for this study

	PDB ID	
receptor	Inactive-like	Active-like
rhodopsin	1GZM-A	2X72
	1U19-A	3PQR
		3PXO
		4A4M
β_2 receptor	2RH1	3P0G
	3D4S	3SN6
	3NY8	
	3NY9	
A_{2A} receptor	3EML	2YDO
	3VG9	2YDV
	4EIY	3QAK

Results

Of all the heptahelical bundles of GPCRs archived on our website (www.gses.jp/7tmsp), we used 18 sets of coordinates in the present study (Table 1), consisting of 9 inactive (2 of rhodopsin, 4 of β_2 receptor, and 3 of A_{2A} receptor) and 9 active-like (4 of rhodopsin, 2 of β_2 receptor, and 3 of A_{2A} receptor) states. All of these structures contain the same sequence ranges of the transmembrane domains superimposed onto the same reference coordinates—the inactive state of β_2 receptor (2RH1)—by secondary structure matching[18]. The aligned structures are shown in Fig. S1. The structural differences between the inactive and active-like states were then analyzed using 8 pairs for rhodopsin, 8 pairs for β_2 receptor, and 9 pairs for A_{2A} receptor. Accordingly, we anticipated that the degree of averaging would be comparable for these 3 receptors. The details of the criteria for the selection of the coordinates are described in the Methods.

Fig. 1 shows the averaged calculated Cα displacement of 200 transmembrane residues between the inactive and active-like states of the 3 receptors. The most prominent feature commonly observed was an oscillating pattern at the cytoplasmic side of helix VI (residue no. 145 ~ 160). Although the magnitude of displacement in this region differs significantly among the receptors, which is most likely due to the current limitation of available crystallization conditions for stabilizing the fully active state for each receptor, the positions of the peaks match well with each other, indicating that similar rotational movement occurs around the axis of this helix upon activation. It is also noteworthy that, at the extracellular side of helix VI (residue no. 160 ~ 176), a significantly larger change occurs in rhodopsin than in β_2 receptor and A_{2A} receptor.

The cytoplasmic side of helix III (residue no. 75 ~ 89) is another region where these receptors exhibit substantial displacement of 1.5 ~ 2 Å, which has been attributed in part to the translational shift toward the extracellular side[5].

By averaging the values for the 3 receptors, structurally conserved residue positions were obtained, as listed in Table S1. Overall, residues around the highly conserved sequence positions (*.50 in Ballesteros-Weinstein [BW] numbering[19], where * is the serial number of helix) in helices I, II, IV, and VI appear to be fixed during activation. In particular, of the most structurally conserved 21 residues, 14 residues are in helix I (1.47, 1.48, and 1.50 ~ 1.54) and II (2.48 and 2.50 ~ 2.55). This finding is consistent with the notion that the so-called N-D pair (side chain interaction between 1.50 and 2.50) in these helices plays an important role as an intramolecular scaffold during activation.

To gain additional insight into the structural changes shown in Fig. 1, we analyzed the axis of each helix III and VI by helanal[20] (Figs S2 and S3). Examples of the inactive states are shown in Fig. 2. Each axis consists of a series of points penetrating about the center of a helix, with the number of points obtained for each axis equal to the number of residues minus 2. Thus, for convenience, we consider that both the N- and C-terminal residues lack the corresponding points (Fig. 2 and 3). As previously described, helix III of inactive rhodopsin is buried more deeply into the core of the heptahelical bundle from the center to the extracellular side than not only in the β_2 and A_{2A} receptors shown here, but also in other receptors of a known structure[17]. It is also noticeable that the extracellular part of this helix in the A_{2A} receptor is significantly distorted in the inactive-like state.

We first examined the traces of all axes and confirmed that assignment of the inactive and active-like states was reasonable for the Protein DataBank (PDB) entries shown in Table 1. The distances of the axis points were then calculated for all possible inactive/active-like pairs of a receptor. The average values are shown in Fig. 3. In the case of helix VI, the pattern of distance plots is consistent with the 3 receptors (Fig. 3, lower). Reflecting the kinked shape in the inactive state and rotational movement around an axis upon activation, a roughly linear increase of displacement occurs toward the cytoplasmic side of this helix in rhodopsin and the β_2 receptor. In contrast,

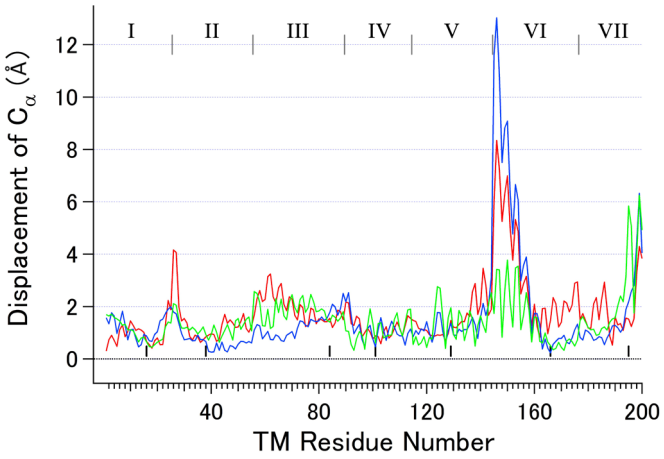

Figure 1 | Averaged displacement (Å) between the inactive and active-like states of the Cα atoms of 200 residues of the 3 receptors. Red: rhodopsin, blue: β_2 receptor, green: A_{2A} receptor. The borders between the adjacent helices are shown with gray bars at the top of the panel, while the positions of seven *.50 residues are shown with short black bars near the zero line of the graph.

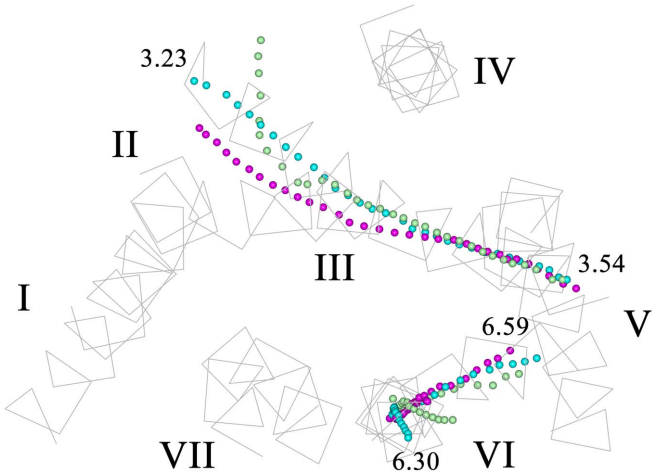

Figure 2 | Projection view of the axis points of helices III and VI in the inactive state from the cytoplasmic side. Magenta: rhodopsin (1U19-A), cyan: β_2 receptor (2RH1), light green: A_{2A} receptor (3VG9). Cα trace of β_2 receptor is also shown in gray. Ballesteros-Weinstein numbers corresponding to the endpoints of the axes are also shown.

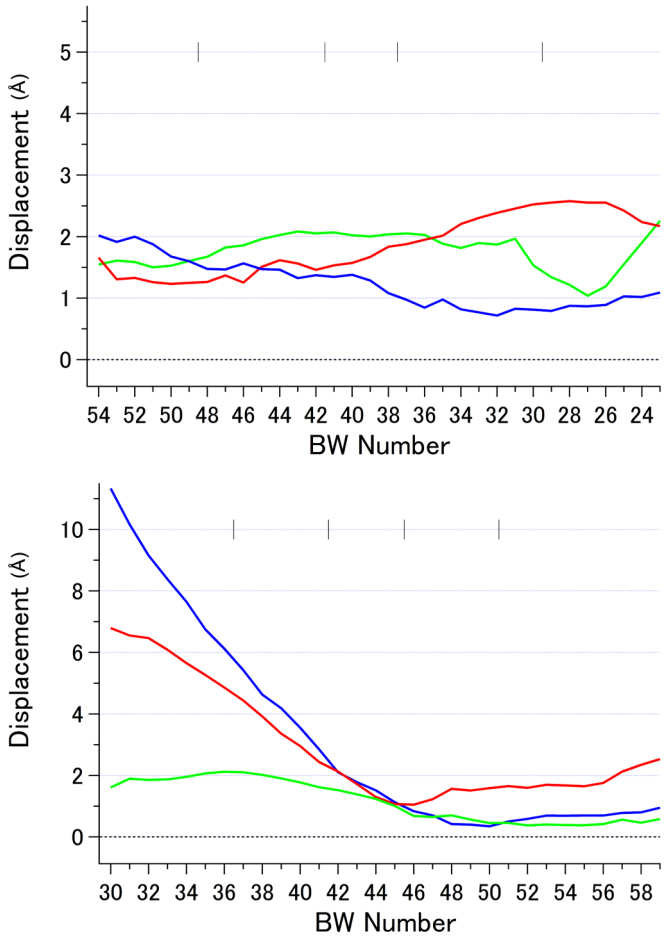

Figure 3 | Averaged difference distance (Å) plot between inactive and active-like states of 3 receptors. Upper: helix III, lower: helix VI. The horizontal axis (BW number) in the upper panel is reversed so that the cytoplasmic side is in the left side of both panels. The borders between the 5 sections stacked along the normal of the membrane plane[17] are shown with gray bars at the top of the panel.

the magnitude of displacement does not change significantly toward the extracellular side. The A_{2A} receptor exhibits a similar pattern of changes, although the increase in the cytoplasmic side is smaller and not linear. Remarkably, the change in the extracellular side of this helix is significantly larger in rhodopsin than in the other 2 receptors, and the point of minimum displacement appears to be shifted from 6.48 ~ Pro6.50 in the β_2 and A_{2A} receptors to 6.44 ~ 6.46 in rhodopsin. As shown in Fig. 2, the inactive backbone of helix III in rhodopsin deviates from the other receptors from ~ 3.40 to the remainder of the extracellular region. Importantly, 3.40 is the position directly in contact with 6.44. These observations suggest that the more buried inactive orientation of helix III and the larger movement in the extracellular side of helix VI are distinct features of rhodopsin, and that while interpreting these, the large differences of the retinal ligand shape and position before and after activation must be considered (see Discussion below).

We also found that the inactive state orientation of helix VI of β_2 receptor is much closer to the active-like helix VI of rhodopsin in the extracellular region than to that of the inactive rhodopsin. This is consistent with the finding that the degree of axis movement in the extracellular side of helix VI upon activation is larger in rhodopsin than in the β_2 receptor.

It has been noted that the activation of GPCRs involves a translational shift of helix III toward the extracellular side[5,12,14]. If the movement of this helix is only translational, the displacement of axis

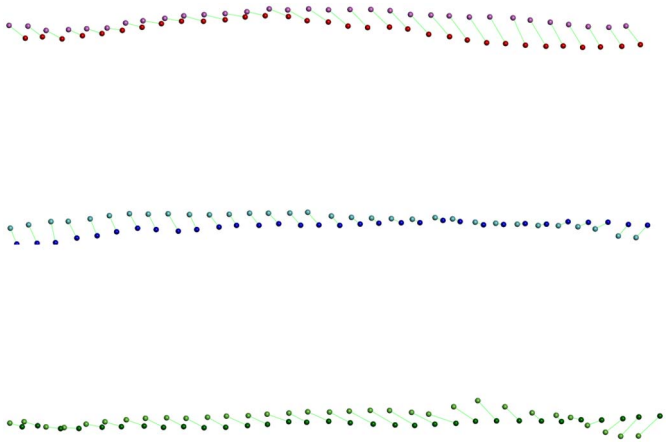

Figure 4 | Changes in the axis points of helix III during the activation of the 3 receptors. Top: rhodopsin. Magenta: inactive (1U19-A), red: active-like (3PXO). Middle: β_2 receptor. Cyan: inactive (2RH1), blue: active-like (3P0G). Bottom: A_{2A} receptor. light green: inactive (3VG9), green: active-like (3QAK). Corresponding axis points in the inactive and active-like states are connected by light green bars.

points would not exhibit a significant change depending on the position in the helix. Fig. 3 (upper panel) shows that the fairly flat pattern observed in the intracellular side is consistent with such a mechanism. However, the change in the pattern of displacement considerably differed among the 3 receptors in the extracellular side. The larger movement observed in rhodopsin is consistent with its distinct arrangement of this helix in the inactive state. On the other hand, an apparently irregular pattern was found in the extracellular side of this helix in the A_{2A} receptor, suggesting that some localized deformation occurred in this region.

To clarify the differences observed between these receptors, representative axes of inactive and active-like helix III are shown in Fig. 4. It is obvious that the translational shift of this helix toward extracellular side appears to be, at least in part, a result of twisting around the long axis. The degree of translation in the cytoplasmic side is likely to be determined by the pattern of twisting, and it varies substantially among the receptors. In the A_{2A} receptor, the pattern of twisting in the cytoplasmic side is distinct from that in the extracellular side (Fig. 4, bottom). In fact, a simple superimposition calculation fails to fit the inactive and active-like axes with each other, suggesting that helix III of the A_{2A} receptor would not behave as a rigid-body during activation.

In order to analyze the rearrangement of helix III in more detail, dihedral angles (Phi, Psi) of each residue were obtained with DSSP[21] (Fig. S4) and then averaged separately for the inactive and active-like helices (Fig. 5). In the A_{2A} receptor, significant changes in the dihedral angles occur at 3.30 ~ 3.31, depending upon the type of the bound ligand. For comparison, the results of a similar calculation for helix VI are shown in Fig. 6. As anticipated from the kinked shape, deviation from the ideal values was observed around 6.48 in the 3 receptors. The angle, however, does not change significantly, regardless of the type of the bound ligand, indicating that this helix behaves almost as a rigid-body in these receptors, as suggested previously[8].

Discussion

The present study is based on the comparison of a similar number of structures (8 ~ 9) for each of the 3 receptors. Although the quality of each structure varies substantially in terms of the claimed resolutions, from 1.8 (4EIY) to 3.5 Å (3P0G), it is unlikely that the findings reported here are affected significantly by such differences, given that we focus only on the backbone rearrangement of the receptors. The possibility that our procedure of fitting of all the inactive and

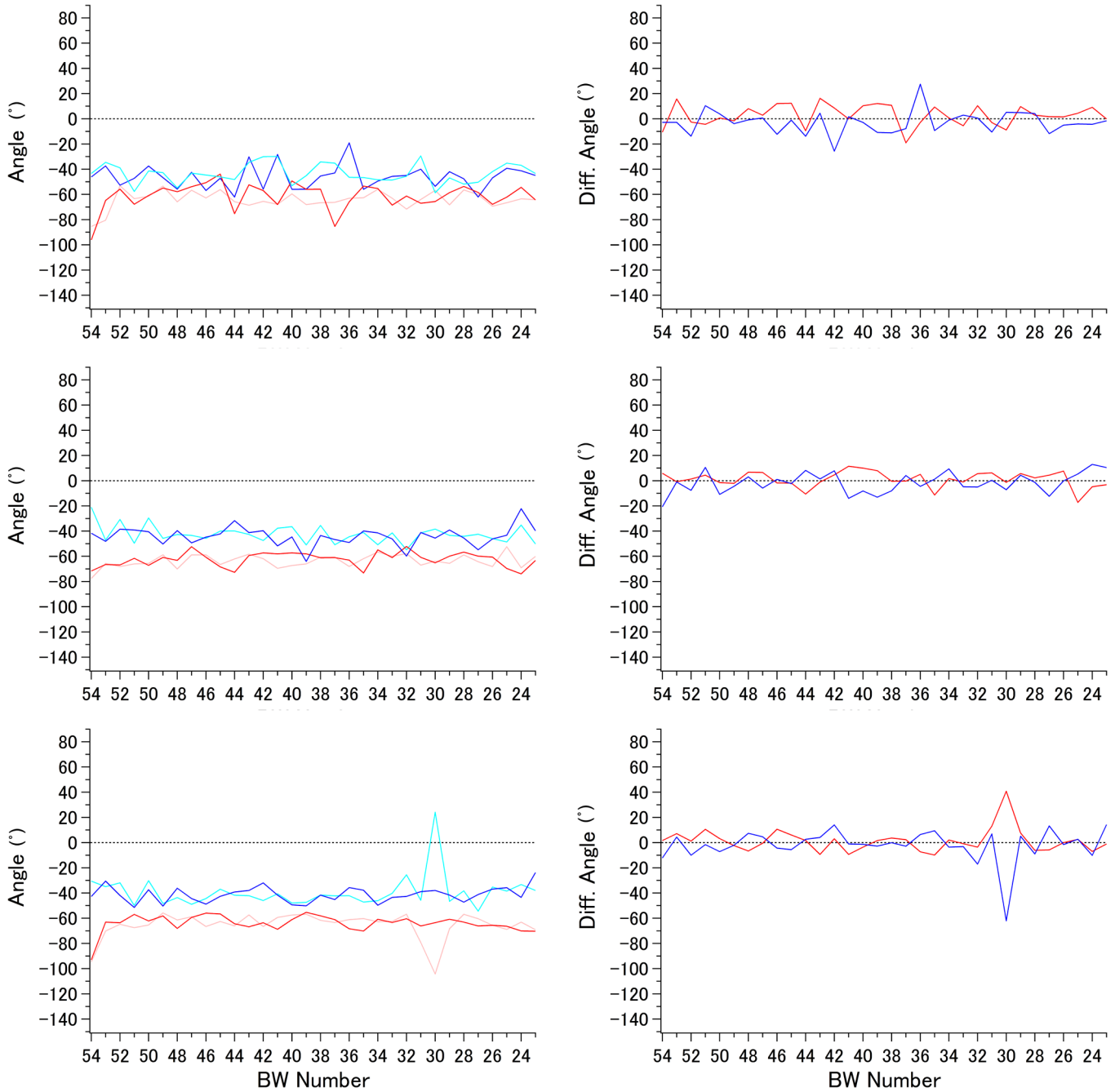

Figure 5 | Phi/Psi (°) plot of helix III. Top: rhodopsin, middle: β_2 receptor, bottom: A_{2A} receptor. Left: averaged Phi/Psi angles; pink: Phi angles of inactive-like states, red: Phi angles of active-like states, cyan: Psi angles of inactive-like states, blue: Psi angles of active-like states. Right: differences between averaged Phi (red), Psi (blue) angles of active-like and inactive-like states.

active-like structures to the inactive β_2 receptor might be inappropriate is also unlikely because we observed the same degree of movements and/or shifts of helices III and VI as those documented in previous crystallographic studies on the activation of the 3 receptors. In addition, the results of fitting independent statistics, such as Phi/Psi angle changes, further validate our procedure of model manipulation.

Given the emerging consensus view that a given GPCR can assume multiple conformational states[1,22], averaging available crystal structure models into 2 states, inactive and active-like, might be valid only for identifying substantial rearrangements of the helices. Nonetheless, our findings suggest that quantitative analyses based on such a 2 state approximation provide detailed information on not only common mechanisms but also receptor-specific mechanisms of activation.

The activity of rhodopsin changes dramatically upon photon absorption, and it is accompanied by the isomerization from 11-*cis* to all-*trans* of a covalently bound retinal ligand. 11-*cis*-retinal is known to act as a strong inverse-agonist, and the differences between the 2 forms of retinal with regard to the shape and position in the binding pocket of opsin are remarkably large compared with ligands bound to other receptors. Therefore, the magnitude of overall rearrangement of the helices in rhodopsin may be larger than the other receptors. This finding is in line with the findings that the displacement in the extracellular side of the helical bundle is larger (Fig. 1), especially in helices III and VI (Fig. 3). Although the plots in

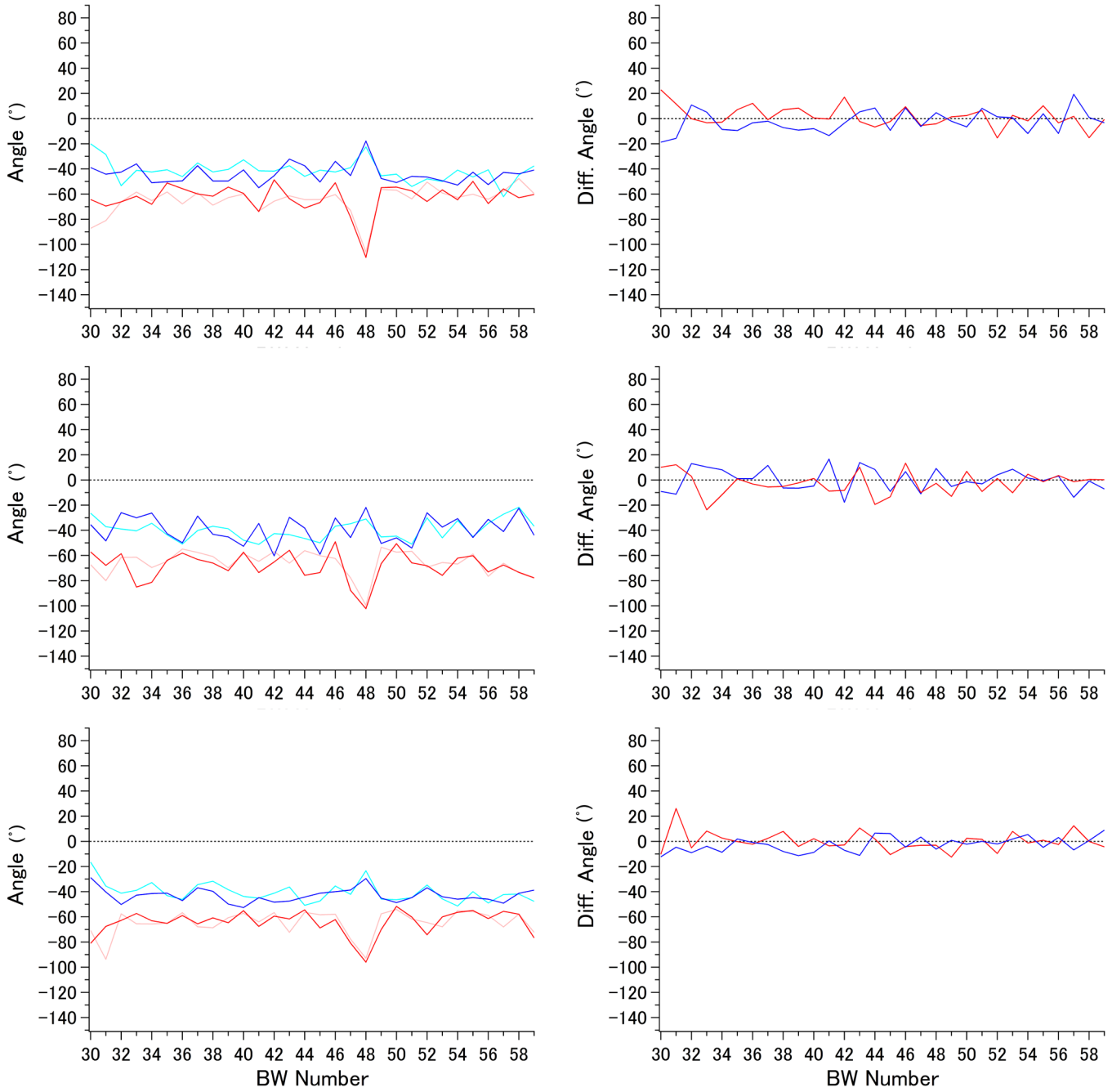

Figure 6 | Phi/Psi (°) plot of helix VI. Top: rhodopsin, middle: β_2 receptor, bottom: A_{2A} receptor. Left: averaged Phi/Psi angles; pink: Phi angles of inactive-like states, red: Phi angles of active-like states, cyan: Psi angles of inactive-like states, blue: Psi angles of active-like states. Right: differences between averaged Phi (red), Psi (blue) angles of active-like and inactive-like states.

Figures 1 and 3 may be influenced by the manner of fitting the multiple structures, the increase in the distance between the 2 helices of rhodopsin at the extracellular side was confirmed by measuring the interhelical Cα distances, which is independent of how active-like structures were fit onto the inactive ones (Fig. S5). We speculate that an extension of such an analysis would be useful for obtaining further insights into the relative positional changes among the 7 helices.

The outstanding local twist of helix III observed in the activation of the A_{2A} receptor is likely to be related to its curved shape in the inactive state, the degree of which is slightly different in the 2 states, namely, with (3VG9) or without (3EML and 4EIY) an inactivating antibody bound at the cytoplasmic side. Therefore, it is likely that the backbone rearrangement upon agonist binding at the extracellular side of this helix would directly affect the interaction with helix VI from the middle to the intracellular side of the membrane.

The Phi/Psi angles of 3.30 ~ 3.31 in the A_{2A} receptor change to a remarkable extent depending on the type of the bound ligand (Fig. 5). The side chains of these 2 residues in the 3 receptors do not point toward the interior of the helical bundle and do not appear to be directly involved in ligand binding. It should be noted that deviations in Phi/Psi angles at these residues from the canonical values are larger in the receptor with an inactivating antibody bound to an intracellular surface than that without it. This observation is in agreement with the finding that the overall twist at the extracellular side of helix III is significantly enhanced in the antibody-bound A_{2A} receptor (Fig. S2). Upon agonist binding, the overall shape of this helix

becomes more like a regular α-helical structure that exhibits little bending. It is likely that there are many other receptors of unknown structure that contain a kink at the extracellular side of helix III in the inactive structure. In such cases, a localized twisting motion would be possible depending on the type of a bound ligand, leading to rearrangement of the short segment in the helix.

In summary, the present study highlights the importance of quantitative analysis of the experimentally available structures to identify common and distinct rearrangement of transmembrane helices induced upon the activation of the 3 members of rhodopsin-like GPCRs. In particular, rearrangement of helix III was found to be a function of the type of receptor. While it has been well recognized that the interaction between this helix and helix VI is a key event in the regulation of the GPCR activity, the mechanism should be considered taking into account the non-rigid-body-like nature of the polypeptide backbone.

Methods

Selection and structural alignment of heptahelical transmembrane bundles were carried out as previously described[17]. Briefly, all the polypeptides from PDB entries were superimposed onto the inactive-like state of β_2 receptor (2RH1) by secondary structure matching[18], and 7 helices consisting of 200 residues were isolated based on unambiguous sequence alignment.

The active-like structures of rhodopsin can be classified into 2 groups, a ligand-free opsin form and an all-*trans*-retinal agonist-bound form. Because the backbone coordinates of these structures are quite similar to each other, we chose only agonist-bound structures for this study. Among the alternatives of inactive structures of the β_2 and A_{2A} receptors, the coordinates listed in Table 1 were selected by taking higher-resolution structures. Of the 3 agonist-bound structures of β_2 receptor reported to date, 3PDS was not used because of its negligible backbone deviation from the inactive-like structure.

DSSP analysis showed that all of the helices III and VI assume regular α-helical secondary structure throughout the entire lengths, with the exception of the cytoplasmic terminals of 3NY8, 3NY9, and 3.30 ~ 3.31 of 3VG9. Therefore, all helices III and VI were analyzed by helanal to determine the axes of the α-helices. Consequently, an axis point corresponding to 3.30 of 3VG9 appeared to be slightly displaced from the expected position within the helix. Although this error does not affect the findings described in this paper, we replaced the coordinate of the point by the averaged values of the preceding and the following points.

Several of the PDB entries contain 2 alternative coordinates for each of a few residues. Because deviations between the 2 Cα positions were negligibly small, we chose conformer A for all cases. Distances between the inactive and active-like axis points were obtained with Chimera[23] and CCP4MG[24] while that of entire heptahelical bundles were calculated by inserting the coordinates in a conventional equation. Phi/Psi angles were obtained by DSSP.

For interhelical Cα distance analysis, the coordinates in the inactive and active-like structures were first averaged separately for each of the 3 receptors, and the intramolecular Cα distances were calculated for all possible pairs in helices III and VI of the averaged inactive and active-like structures. The differences of the distances at each pairs of positions were then obtained between the inactive and active-like structures.

All graphs were prepared with IgorPro (WaveMetrics), and the remaining figures were prepared with CCP4MG[24] and Discovery Studio Visualizer (Accelrys).

1. Kobilka, B. K. & Deupi, X. Conformational complexity of G-protein-coupled receptors. *Trends Pharmacol. Sci.* **28**, 397–406 (2007).
2. Farrens, D. L., Altenbach, C., Yang, K., Hubbell, W. L. & Khorana, H. G. Requirement of rigid-body motion of transmembrane helices for light activation of rhodopsin. *Science* **274**, 768–770 (1996).
3. Park, J. H., Scheerer, P., Hofmann, K. P., Choe, H. W. & Ernst, O. P. Crystal structure of the ligand-free G-protein-coupled receptor opsin. *Nature* **454**, 183–187 (2008).
4. Rasmussen, S. G. *et al.* Structure of a nanobody-stabilized active state of the β(2) adrenoceptor. *Nature* **469**, 175–180 (2011).
5. Xu, F. *et al.* Structure of an agonist-bound human A_{2A} adenosine receptor. *Science* **332**, 322–327 (2011).
6. Hirai, T., Subramaniam, S. & Lanyi, J. K. Structural snapshots of conformational changes in a seven-helix membrane protein: lessons from bacteriorhodopsin. *Curr Opin Struct Biol.* **19**, 433–439 (2009).
7. Choe, H.-W. *et al.* Crystal structure of metarhodopsin II. *Nature* **471**, 651–655 (2011).
8. Standfuss, J. *et al.* The structural basis of agonist-induced activation in constitutively active rhodopsin. *Nature* **471**, 656–660 (2011).
9. Deupi, X. *et al.* Stabilized G protein binding site in the structure of constitutively active metarhodopsin-II. *Proc Natl Acad Sci USA* **109**, 119–124 (2012).
10. Warne, T. *et al.* The structural basis for agonist and partial agonist action on a β(1)-adrenergic receptor. *Nature* **469**, 241–244 (2011).
11. Søren, G. F. *et al.* Crystal structure of the β_2 adrenergic receptor–Gs protein complex. *Nature* **477**, 549–555 (2011).
12. Lebon, G. *et al.* Agonist-bound adenosine A_{2A} receptor structures reveal common features of GPCR activation. *Nature* **474**, 521–525 (2011).
13. White, J. F. *et al.* Structure of the agonist-bound neurotensin receptor. *Nature* **490**, 508–513 (2012).
14. Hulme, E. C. GPCR activation: a mutagenic spotlight on crystal structures. *Trends Pharmacol Sci.* **34**, 67–84 (2013).
15. Lebon, G., Warne, T. & Tate, C. G. Agonist-bound structures of G protein-coupled receptors. *Curr Opin Struct Biol.* **22**, 482–490 (2012).
16. Unal, H. & Karnik, S. S. Domain coupling in GPCRs: the engine for induced conformational changes. *Trends Pharmacol Sci.* **33**, 79–88 (2012).
17. Okada, T. Comparative analysis of the heptahelical transmembrane bundles of G protein-coupled receptors. *PLoS One* **7**, e35802 (2012).
18. Krissinel, E. & Henrick, K. Secondary-structure matching (SSM), a new tool for fast protein structure alignment in three dimensions. *Acta Crystallogr* **D60**, 2256–2268 (2004).
19. Ballesteros, J. A. & Weinstein, H. Integrated methods for the construction of three-dimensional models and computational probing of structure-function relations in G protein-coupled receptors. *Methods Neurosci* **25**, 366–428 (1995).
20. Bansal, M., Kumar, S. & Velavan, R. HELANAL: a program to characterize helix geometry in proteins. *J Biomol Struct Dyn* **17**, 811–819 (2000).
21. Kabsch, W. & Sander, C. Dictionary of protein secondary structure: pattern recognition of hydrogen-bonded and geometrical features. *Biopolymers* **22**, 2577–2637 (1983).
22. Kenakin, T. Ligand-selective receptor conformations revisited: the promise and the problem. *Trends Pharmacol Sci.* **24**, 346–54 (2003).
23. Pettersen, E. F. *et al.* UCSF Chimera--a visualization system for exploratory research and analysis. *J Comput Chem* **25**, 1605–1612 (2004).
24. McNicholas, S., Potterton, E., Wilson, K. S. & Noble, M. E. M. Presenting your structures: the CCP4mg molecular-graphics software. *Acta Cryst* **D67**, 386–394 (2011).
25. Wang, C. *et al.* Structural basis for molecular recognition at serotonin receptors. *Science* **340**, 610–614 (2013).
26. Wacker, D. *et al.* Structural Features for Functional Selectivity at Serotonin Receptors. *Science* **340**, 615–619 (2013).

Acknowledgments

Supported by the Ministry of Education, Culture, Sports, Science and Technology of Japan.

Author contributions

S.N., T.I., D.O. performed analysis, T.O. designed research, performed analysis, and wrote the manuscript.

Additional information

Supplementary information accompanies this paper at http://www.nature.com/scientificreports

Competing financial interests: The authors declare no competing financial interests.

How to cite this article: Nakamura, S., Itabashi, T., Ogawa, D. & Okada, T. Common and distinct mechanisms of activation of rhodopsin and other G protein-coupled receptors. *Sci. Rep.* **3**, 1844; DOI:10.1038/srep01844 (2013).